Journal of Materials Chemistry B

ROYAL SOCIETY OF CHEMISTRY

PAPER

View Article Online
View Journal | View Issue

Cite this: J. Mater. Chem. B, 2023, 11, 2927

Swelling induced mechanically tough starch–agar based hydrogel as a control release drug vehicle for wound dressing applications

Dimpee Sarmah,[a] Munmi Borah,[b] Manabendra Mandal[b] and Niranjan Karak *[a]

In recent years, polysaccharide-based hydrogels have received increased attention due to their inherent biodegradability, biocompatibility, and non-toxicity. The feasibility of using polysaccharides for the synthesis of hydrogels is dependent on their noteworthy mechanical strength and cell compatibility, which are required for practical applications, especially for biomedical uses. In this study, we demonstrate a facile synthetic route for the construction of a mechanically tough, biocompatible, and biodegradable hydrogel using polysaccharides such as starch and agar. A synthetic monomer-free hydrogel was synthesized using epichlorohydrin as a cross-linker, and a mechanical strength of 9.49 ± 1.29–6.16 ± 0.37 MPa was achieved. The introduction of agar into the hydrogel resulted in agar dose-dependent swelling-induced mechanical strength. Moreover, along with incredible mechanical strength, the hydrogel also exhibited prominent cell viability against human embryonic kidney cells. In addition, the hydrogel showed good encapsulation efficiency for antibacterial drugs like ciprofloxacin hydrochloride hydrate, with controlled releasing ability over a sustained period. The antibacterial activity of the encapsulated drug was observed against *Staphylococcus aureus* and *Bacillus subtilis* bacterial strains. Thus, the studied hydrogel with loaded drug exhibited all the required qualities to be utilized as a promising candidate in wound dressing applications.

Received 22nd December 2022,
Accepted 27th February 2023

DOI: 10.1039/d2tb02775e

rsc.li/materials-b

Introduction

Skin is a protective layer of human and animal bodies and plays an imperative role in containing bodily fluids, nutrients, electrolytes, *etc.*[1] Skin wounds are one of the most frequent and common injuries that lead to bacterial infections and serious tissue damage.[2] Covering the damaged skin with a suitable dressing material is one of the most effective ways to prevent bacterial invasion. Among the recently reported dressing materials, hydrogels, three-dimensionally cross-linked highly hydrophilic soft and wet polymeric materials, have received increased attention in medicinal chemistry. Along with their inherent hydrophilicity, the biocompatible nature, permeability, and low frictional coefficient, *etc.*, of hydrogels make them suitable for use in biomedical applications.[3] Among their various biomedical applications, hydrogels have shown great applicability as wound dressing materials due to their high absorption capacity for blood, exudates, *etc.*, eliminating the frequent need to replace dressing materials.[4] Moreover, hydrogels can maintain a moist environment in the affected area to promote fast wound healing. In addition to this, the soft texture of hydrogels resembles the extracellular matrix, and the porous network aids oxygen transportation to the wound.

However, in comparison with other polymeric materials, hydrogels exhibit lower mechanical strength because of their structural inhomogeneity or requirement of effective energy dissipation mechanisms.[5] This inherent drawback limits the practical applicability of hydrogels in different fields, including wound dressing applications. Over the last few decades, a number of studies have reported mechanically tough hydrogels for dressing applications. For example, in 2017, a pH responsive tough hydrogel was synthesized as a smart dressing material by Liu *et al.* The hydrogel was synthesized by using sodium alginate, and acryl amide was used as a synthetic monomer.[6] In 2020, a highly stretchable mechanically tough poly(sulfobetaine methacrylate) hydrogel was synthesized by Fang *et al.* The mechanoresponsive hydrogel showed good adhesive properties, exhibiting 1.41 MPa compressive stress.[7] Recently, a highly stretchable hydrogel was also synthesized using acrylamide as a monomer and *N,N*-bis(acryloyl)cysteamine as the cross-linking agent.[8]

Although all these hydrogels have shown potential as effective mechanically tough dressing materials, the use of synthetic monomers limits their applicability. Thus, in this work we

[a] *Advanced Polymer & Nanomaterial Laboratory, Department of Chemical Sciences, Tezpur University, Tezpur 784028, Assam, India. E-mail: karakniranjan@gmail.com*
[b] *Department of Molecular Biology and Biotechnology, Tezpur University, Napaam, Tezpur, 784028, Assam, India*

aimed to synthesize a polysaccharide-based synthetic monomer-free hydrogel by using starch and agar. Starch is one of the most abundant plant-derived polysaccharides, containing large numbers of glucose units joined *via* α-d-(1–6) and/or α-d-(1–4) linkages.[9] Starch contains two major components: amylose and amylopectin. Different proportions of these two constituents affect the overall crystallinity, gelatinization process, and molecular order of the starch. The highly reactive primary hydroxyl groups present in starch molecules can be used to cross-link by using various cross-linking agents. In this vein, agar is a unique gel-forming polysaccharide containing alternating-(1–4)-D-galactose and-(1–3)-3, 6-anhydro-L-galactose units.[10] Upon exposure to heat, agar can undergo melting, reset on cooling, and these processes can be carried out for infinite cycles. However, literature advocates the preparation of different polysaccharide-based mechanically tough hydrogels. Each of these possesses a definite amount of swelling ability. During swelling, hydrogels expand their 3D network, and thus, most of them suffer from a swelling-induced decline in mechanical properties.[11] Moreover, several hydrogels after equilibrium absorption are unable to retain their structural integrity, and this leads to serious performance issues. Although extensive studies have reported various hydrogels with different swelling abilities, only a few of them have reported a retention of mechanical properties both before and after swelling. This may be due to the fact that most of them are too weak after swelling. However, a few literature studies have reported that hydrogels show noticeable mechanical strength after swelling, for example, Itagaki *et al.* reported a poly(2-acrylamido-2-methylpropanesulfonic)/polyacrylamide-based hydrogel with retention of mechanical strength after swelling.[12] Similarly, Wang *et al.* synthesized a poly(*N*-isopropylacrylamide) and a LAPONITE®-based nanocomposite with noticeable mechanical strength after swelling.[13] Although these hydrogels can retain the mechanical strength after swelling, their applicability is limited due to the use of synthetic monomers. Thus, designing a bio-based hydrogel with strong mechanical attributes, both in the dry and swollen states, is still a big challenge.

In this study, we aimed to produce a mechanically tough polysaccharide-based hydrogel with retention of its swelling-induced mechanical properties. To cross-link the polysaccharides starch and agar, epichlorohydrin (ECH) was used as a cross-linker and different compositions of the hydrogels with varying mechanical performances were prepared. The antibacterial drug ciprofloxacin was encapsulated within the hydrogel and the antibacterial efficiency of the drug-loaded hydrogel was tested against both Gram-positive and Gram-negative bacteria. Moreover, the controlled release attributes of the hydrogel were investigated *in vitro* to understand the release profile for the sustained release of drug. Most importantly, to examine the toxicity of the hydrogel towards mammalian cells, cell viability tests were also conducted.

Experimental

Materials and methods

Tapioca starch was received from Hindustan Gum & Chemicals Ltd, India. Agar powder, phosphate-buffered saline (PBS), and Luria-Bertani broth growth media were purchased from Himedia, India. ECH was purchased from SRL, India. Ciprofloxacin hydrochloride hydrate was obtained from SRL, India.

Sodium dodecyl sulfate (SDS), Luria-Bertani, crystal violet, and 3-(4,5-dimethylthiazol-2-yl)-2,5-diphenyltetrazolium bromide (MTT) were procured from Himedia, India. Dulbecco's modified Eagle's medium, non-essential amino acids, penicillin-streptomycin solution, L-glutamine, foetal bovine serum, and 4-(2-hydroxyethyl)-1-piperazineethanesulfonic acid were purchased from Sigma, Germany.

Gram-positive bacteria, such as *Staphylococcus aureus* (SA) (MTCC 3160) and *Bacillus subtilis* (BS) (MTCC 121), were obtained from Microbial Type Culture Collection, CSIR Institute of Microbial Technology, Chandigarh, India. All the bacterial strains were cultured for 24 h in Luria-Bertani (LB) broth.

Synthetic procedure

The starch–agar-based mechanically tough hydrogel was synthesized *via* a facile one-pot procedure. Calculated amounts of starch and agar powder were placed in a round-bottom flask with distilled water. The reaction temperature was gradually increased under stirring up to 70–80 °C to dissolve both the polysaccharides. Thereafter, the temperature of the reaction mass was lowered to 60 °C and at that temperature, the desired amount (0.7185 g) of ECH was added dropwise with the subsequent addition of 3 N NaOH solution. The reaction mixture was stirred until all the NaOH had reacted with the ECH as indicated by the increase in the viscosity of the reaction mixture. The viscous gel was then poured onto a Teflon sheet and dried in an oven at 50 °C until a touch-free film of the hydrogel formed. Materials with different molar ratios of starch and agar were prepared, encoded as SAC1, SAC2, and SAC3, as tabulated in Table 1.

Table 1 Concentration of reactants used in the synthesis of the hydrogel

	Starch		Agar		ECH		
Sample code	Amount (g)	Concentration (g/100 mL)	Amount (g)	Concentration (g/100 mL)	Amount (g)	Concentration (g/100 mL)	Water content (mL)
SAC1	1.4	9.33	0.1	0.66	0.7185	4.79	15
SAC2	1.2	8	0.3	2	0.7185	4.79	15
SAC3	1	6.66	0.5	3.33	0.7185	4.79	15

Fourier-transform infrared (FT-IR) spectroscopy study

The FTIR spectra of starch, agar, and the synthesized hydrogels were recorded over a wavenumber range of 4000 to 400 cm^{-1} using an FTIR spectrometer (Impact-410, Madison, WI).

Thermal study

The thermogravimetric analyses (TGA) of the hydrogels were conducted on a TGA-4000 (PerkinElmer) instrument within a temperature range of 32–720 °C at a 10 °C min^{-1} heating rate under a N_2 atmosphere with a 30 mL min^{-1} flow rate. Before analysis, the hydrogels were oven dried at 50 °C under vacuum to eliminate the water present in the samples.

Mechanical testing

To determine the tensile strength of the hydrogel films a universal testing machine (UTM) (Model WDW-10, Jinan, China) was used. In all the measurements, a 1.0 kN load cell was used with a 5 mm min^{-1} crosshead speed.

Water absorption capacity

To evaluate its swelling ability, a predetermined amount of the hydrogel was immersed in PBS. Before immersion, the hydrogel film samples were oven dried to a constant weight. The swollen gels at equilibrium were taken from the liquid medium, the loosely adhered water was removed, and their final weight was taken. The following relationship was used to determine the swelling ability of the hydrogels:

$$\text{Swelling} = (W_t - W_i)/W_i \quad (1)$$

where W_t is the weight of the equilibrium swollen gel and W_i is the initial weight of the dry hydrogel.[14]

The tensile strength was also measured under swollen conditions. To determine the tensile strength of water-absorbed hydrogels, the same UTM machine was used under similar conditions as done for the dry hydrogel films. Moreover, the tensile strengths of the swollen hydrogel were measured both in a fully swollen state and containing around 70% water.

Water vapor transmission rate (WVTR)

The WVTR of the SAC3 hydrogel was evaluated following ASTM standard E96-00 with slight modification.[15] A salt solution of calcium chloride and sodium chloride with 2.5 mmol L^{-1} calcium ions and 142 mmol L^{-1} sodium ions (equivalent to the chemical composition of wound fluid and serum) was taken up in a glass vial. The mouth of the vial was covered with hydrogel film, ensuring contact with the water present inside the vial. The mouth of the vial was closed using a Teflon tap so that the vapor could escape only through the hydrogel film. Thereafter, the vial was sealed with the test sample incubated at 37 °C temperature, and the weight of the container was measured at regular time intervals (6, 12, 18, 24 h) and an average of three consecutive test results was taken. The equation used to evaluate the WVTR of SAC3 was as follows:

$$\text{WVTR} = (m/t)\ 24/A\ (\text{g m}^{-2}\ \text{d}^{-1}) \quad (2)$$

where m = the mass of water loss after a particular time interval (g), t = time interval (h), and A = the effective transfer area of the hydrogel (m^2).[16]

Ciprofloxacin loading

Before encapsulation, different amounts of drug were dissolved in distilled water and mixed with the produced gel after the completion of the reaction. Thereafter, the drug-loaded gel was dried in an oven at 50 °C until the formation of a touch-free film.

To determine the encapsulation efficiency of the SAC3, at first the loosely adhered drug was removed by washing with distilled water. The loosely attached drug was determined by measuring the concentration of the drug in the water washings using a UV-visible spectrophotometer at the λ_{max} (270 nm) of ciprofloxacin. A standard curve prepared using known concentrations of ciprofloxacin hydrochloride hydrate was used to determine the amount of the drug in water. The following equation was used to determine the encapsulation efficiency of the hydrogel:

$$\text{Encapsulation efficiency (\%)} = (Q_0 - Q_r) \times 100/Q_0 \quad (3)$$

where Q_0 is the initial amount of the drug and Q_r is the amount of the drug in the filtrate.[17]

The percent of drug loading was determined with the help of the equation:[18]

$$\text{Ciprofloxacin loading (\%)} = (\text{weight of drug in the hydrogel/weight of the hydrogel}) \times 100 \quad (4)$$

In vitro drug release study

For *in vitro* release study, the ciprofloxacin loaded hydrogel films were placed in a definite amount of PBS solution at 37 °C. After predetermined time intervals, 1 mL of drug release buffer was collected. After diluting the drug release buffer by an appropriate amount, the absorbance of the released drug was evaluated by using a UV-vis spectrophotometer at the λ_{max} (270 nm) of ciprofloxacin. For the determination of the concentration of the drug, a standard curve was created in the same way as for the loading efficiency of the hydrogel. To determine the cumulative drug release (%), the following equation was used:

$$\text{Cumulative release (\%)} = (M_t/M_0) \times 100\% \quad (5)$$

where M_t is the drug release at time t and M_0 is the initially loaded drug.[18]

Biodegradation *via* the soil burial method

The soil burial method was used to investigate the biodegradation of the synthesized hydrogel. Weighed amounts of hydrogel samples without the incorporation of drug were taken up in paper cups containing 40 g of soil with 30 mL of water. Thereafter, all the cups were buried under soil of 6–8 cm in depth. After a specific time interval, the hydrogels were collected from the soil and washed gently using water to eliminate the adhered

soil. The degraded samples were then air dried, and their respective weights were taken. The weight loss after degradation was calculated by using the following equation:

$$\text{Weight loss (\%)} = (\text{weight of the hydrogel before degradation} - \text{weight of the hydrogel after degradation})/\text{weight of the hydrogel before degradation} \times 100 \quad (6)$$

The change in the surface morphology after biodegradation was analyzed by scanning electron microscopy (JSM 6390LV, Japan).

Antimicrobial testing of the drug loaded hydrogel

The antimicrobial activity of the drug-loaded hydrogel was determined using agar well diffusion methods. The bacterial strains taken for analysis were cultured overnight. An amount of 100 μL of each of the bacterial cultures was spread evenly on the Luria-Bertani agar surface. Wells were created with the help of a 6 mm metallic borer. SAC3 without drug, drug encapsulated SAC3, and ciprofloxacin as the positive control were added to each of the plates and incubated overnight at 37 °C. The plates were screened to determine the inhibition zone (in mm) of each sample.[19]

Cytotoxicity studies of the hydrogel on human embryonic kidney cells (HEK 293)

Dulbecco's modified Eagle's medium was used to culture the human embryonic kidney cells (HEK 293). The medium was supplemented with 1% penicillin–streptomycin solution, 10% foetal bovine serum, 0.05% L-glutamine, 0.6% 4-(2-hydroxyethyl)-1-piperazineethanesulfonic acid, and 1% non-essential amino acids. To evaluate the cytotoxicity of the hydrogel, 1×10^4 HEK293 cells were grown for 24 h in the well of a 96-well plate at 37 °C with 5% CO_2 prior to the addition of SAC3. Thereafter, the cells were treated with different concentrations of the hydrogel (without drug), and the cell morphology was studied using an inverted microscope (ZEISS, Model Axio Vert. A1). For cell viability study, after 24 h of incubation with the synthesized hydrogel, the cells were treated with MTT solution at 37 °C for 4 h in a cell culture incubator (Eppendorf Galaxy 170). In the case of metabolically active cells, due to mitochondrial dehydrogenases, MTT was converted to an insoluble dark purple formazan. A denaturing buffer solution containing HCl, SDS, and isopropanol was used to dissolve the formazan crystals. The absorbance was evaluated using a 96-well plate reader (Thermo Scientific Multiskan GO) at a wavelength of 570 nm.[20] The cell viability was evaluated using the following equation:[21]

$$\text{Cell viability (\%)} = \text{absorbance of the treated well/absorbance of the untreated well} \times 100 \quad (7)$$

Results and discussion

Synthesis of the hydrogel

The possible synthetic pathway for the starch–agar-based mechanically tough hydrogel is demonstrated in Scheme 1. In a basic environment, the epoxy rings of ECH were opened and reacted with one of the primary hydroxyl groups of the starch molecules. Consequently, another primary hydroxyl group of starch reacted with the other side of the opened-up epoxy ring of ECH. Moreover, the opened epoxy ring can also react with the primary hydroxyl groups of agar and starch simultaneously, and, thus, the starch–agar cross-linked hydrogel was formed, as depicted in Scheme 1.

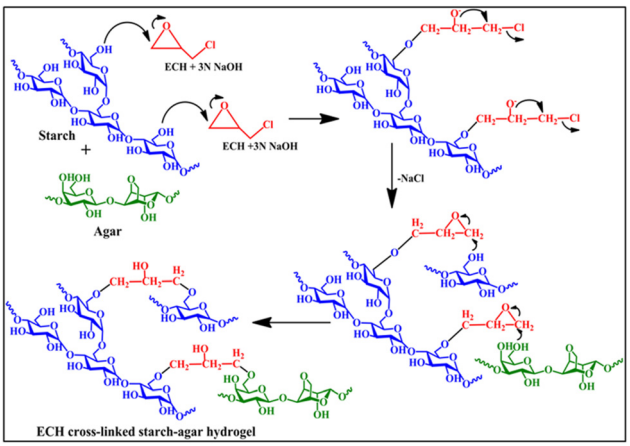

Scheme 1 Possible reaction mechanism for the preparation of the hydrogel.

FTIR spectroscopy study

The characterization of the synthesized hydrogel was done using FT-IR spectroscopy analysis. The FT-IR spectra of starch, agar, and all the hydrogels are shown in Fig. 1(a) and (b).

The spectra clearly provide evidence for the ECH cross-linking with the polysaccharides. The absence of an epoxy peak at around 853.88 cm^{-1} and the C–Cl peak at 758.83 cm^{-1} in the spectra of the resulting hydrogels provides evidence for the opening of the epoxy ring of ECH.[22] This observation was also found in our previous work.[23] In addition to this, the decrease

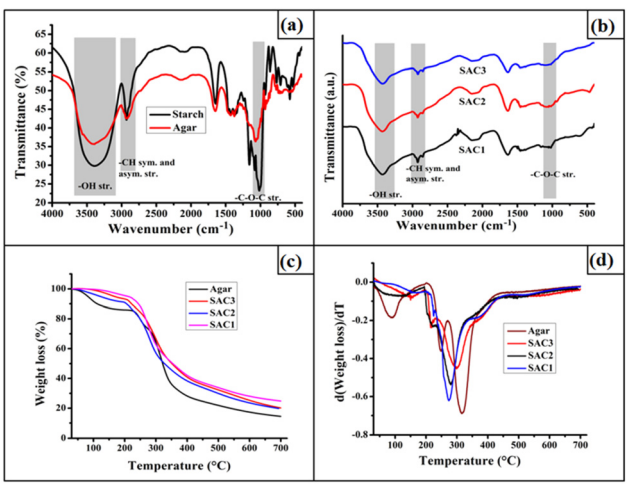

Fig. 1 FTIR spectra of (a) agar and starch; (b) SAC1, SAC2, and SAC3, (c) TGA thermograms of agar and SAC3, and (d) first derivative TG (DTG) of agar and SAC3.

in the broadness of the –OH stretching frequency at 3300–3525 cm^{-1} in the spectra of the synthesized hydrogels revealed the decrease in the degree of free hydroxyl groups in the polysaccharides after ECH cross-linking.[3,24] All three compositions of the hydrogels exhibited an –OH stretching frequency at this wavelength range. The characteristic bands for the –CH symmetric and asymmetric stretching frequencies in the range of 2848.15–2976.05 cm^{-1} were present in both the bare polysaccharides and the resulting hydrogel.[25] Moreover, the characteristic band in the range of 1015.42 cm^{-1} –1166.65 cm^{-1} represents the –C–O–C– stretching frequency of both the starch and agar of the resulting hydrogel.

Thermal study

The TGA thermograms and their first derivatives obtained from the thermal studies of the pristine agar and all three compositions of the hydrogels are shown in Fig. 1(c and d). Both the pristine agar and starch–agar films exhibited multistep degradation patterns during thermal decomposition. The first weight loss is due to the loss of moisture entrapped within the agar powder and the hydrogel matrices. In the case of bare agar, in addition to the weight loss due to water vapor, two weight losses were observed at around 248 °C and 316 °C. These two weight losses were also observed for the synthesized hydrogels. However, the degradation pattern observed at 248 °C for the agar backbone was slightly shifted to 219 °C. However, the intensity of this degradation pattern was much lower for SAC1 compared to SAC3, reflecting the lower agar content in the structure. In addition to this, the degradation pattern observed at around 316.23 °C is due to the decomposition of both the bare starch and bare agar backbones, which were also observed for all three hydrogels with some shifting towards lower temperatures.[25,26] Thus, from this study, it was found that, compared with the bare polysaccharides, the hydrogel films show slightly lower thermal stability.

Swelling study

Swelling is one of the most important properties of hydrogel for wound dressing, as it provides a moist environment for the wounded tissue.[4] A hydrogel with a balanced swelling ability can cool down the wounded area and provide a comparatively comfortable environment to the host. Moreover, the hydrogel can absorb the exudates from the wound site, which is one of the most important properties for successful wound healing. The effluence from the wound enhanced the probability of bacterial colonization and thus delayed the healing process.[27] The developed hydrogel exhibited a swelling ratio of 2.53 ± 0.45 g g^{-1}-6.167 ± 0.40 g g^{-1} in PBS, as shown in Fig. 2(a). The hydrogel with a higher starch amount exhibited higher swelling ability. Moreover, an increase in the amount of agar effectively decreased the water absorption capacity. This phenomenon occurs due to the lower hydrophilicity of agar compared to starch as a result of the presence of fewer hydroxyl groups.

WVTR

Wound healing is a complicated pathophysiological process that requires a suitable moist environment for effective healing.

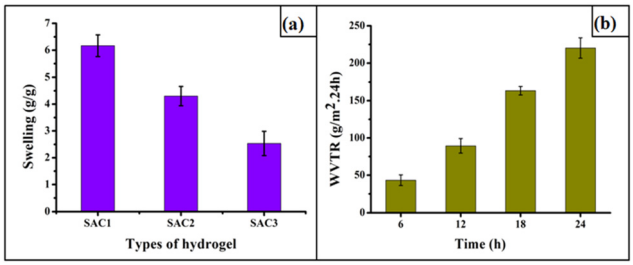

Fig. 2 (a) Swelling of the hydrogels and (b) the water transmission rate of SAC3.

The injured cell exhibits around twenty times higher water loss than normal skin. It has been reported that healing under suitable moist conditions is faster than under dry conditions. Thus, a suitable dressing material is essential for controlling the water evaporation from the wounded area. The water vapor transmission rate of the SAC3 hydrogel film over 24 h is shown in Fig. 2(b). It can be observed that, even if the liquid is in contact with the hydrogel, less water is evaporated, which confirms the synthesized hydrogel to be an effective dressing material.

Mechanical properties

In the biomedical field, acute wounds on body parts such as knees, fingers, feet, and wrists are difficult to treat due to their frequent movements. Therefore, it is highly recommended that the dressing materials to be used for such specific sites should have adequate mechanical strength. Thus, in this work, a mechanically tough hydrogel was prepared to achieve the required mechanical properties for dressing applications.

Taking advantage of the cross-linking of both starch and agar moieties by ECH, the synthesized hydrogel films attained excellent mechanical strength. The typical stress–strain profiles for all three compositions of the hydrogel are shown in Fig. 3(a). The tensile strength of SAC1 was measured as 9.49 ± 1.29 MPa. In contrast, the stresses of SAC2 and SAC3 were measured as 6.99 ± 0.29 MPa and 6.16 ± 0.37 MPa. Thus, compared to SAC1, the difference between SAC2 and SAC3 is small. These results suggest that the incorporation of agar into the ECH cross-linked starch network affects the mechanical strength of the gels. This may be due to the incorporation of agar resulting in less cross-linking, which may lead to the lower

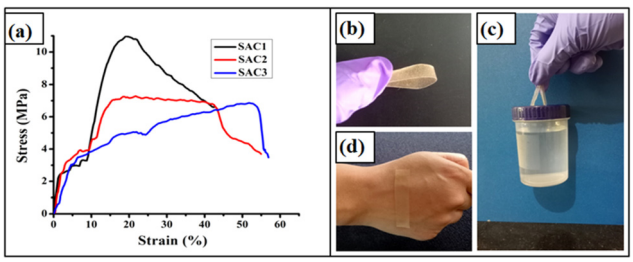

Fig. 3 (a) Stress–strain curves of the hydrogels, (b) bending of the hydrogel, (c) weight lifting, and (d) visual inspection of the skin through the hydrogel film.

mechanical strength of the hydrogels. Moreover, there are possibilities of starch–starch, and agar–starch cross-linking with the opened-up epoxy ring of ECH. Thus, the penetration of both networks together reduced the tensile strength of the resulting hydrogel. However, the difference was not very pronounced in the case of SAC2 and SAC3 in the dry state, as shown in Fig. 3(a).

Further, to provide supportive information for the mechanical strength of the gel, various digital photographs were taken, as shown in Fig. 3(b). It can be observed from the figure that the SAC3 hydrogel can be easily bent without any deformation, which provides support for the prominent mechanical strength of the gel. Further, the mechanical strength of the hydrogel was also evaluated by lifting a plastic bottle filled with water with a weight of 135 g using a strip of the hydrogel. It can be seen from Fig. 3(c) that only 0.1 g of hydrogel can hold almost 135 g of weight without any breakage.

Thus, all these results provide supportive evidence for the mechanical toughness of the synthesized hydrogel. Moreover, the synthesized hydrogel is also transparent enough for visual inspection of the wound through the hydrogel film without removing it, as shown in Fig. 3(d).

Mechanical strength after swelling

Along with the high mechanical strength under dry conditions, the synthesized hydrogel can retain its integrity in the swollen state and possess a noticeable amount of tensile strength both in the fully swollen state and with ~70% absorbed water. However, the SAC1 hydrogel possessing the lowest agar content was not suitable for carrying out the mechanical strength testing in the UTM machine. The stress–strain curves for the swollen hydrogels are shown in Fig. 4(a) and (b). From this figure, it can be clearly observed that SAC3 exhibited a higher tensile strength than SAC2 in both cases. Thus, the noticeable amount of mechanical stability is due to the presence of agar and this property makes the hydrogel suitable for use in dressing applications. To support this fact, gelatinized agar was dried in an oven to a constant weight and kept in water. It can be observed that the dried agar retains its integrity even after 7 days in water, as shown in Fig. 4(c) and (d). Thus, the presence of agar is responsible for the retention of mechanical strength after swelling, which is also predicted from the tensile strength of the swollen gel. However, in the case of the fully swollen state, much lower tensile strength was observed than in the 70% swollen state, as expected.

The digital photographs of all three compositions of the hydrogels after water absorption are shown in Fig. 4(e). Moreover, the SAC3 hydrogel in the swollen state can also bend or twist or form a knot, as shown in Fig. 4(f) and (g).

Thus, all these results prove that the hydrogels have a considerable amount of mechanical strength in the swollen state and that this property arises due to the presence of agar in the network. However, a significant decline in mechanical strength was observed after the absorption of water. This may be due to enhancement in the volume of the hydrogel network by the absorbed water resulting in a lowering of the gel strength. In addition, the hydrophilic groups combined with the water molecules result in decrease of the interactions between the molecular chains present in the hydrogel.[28]

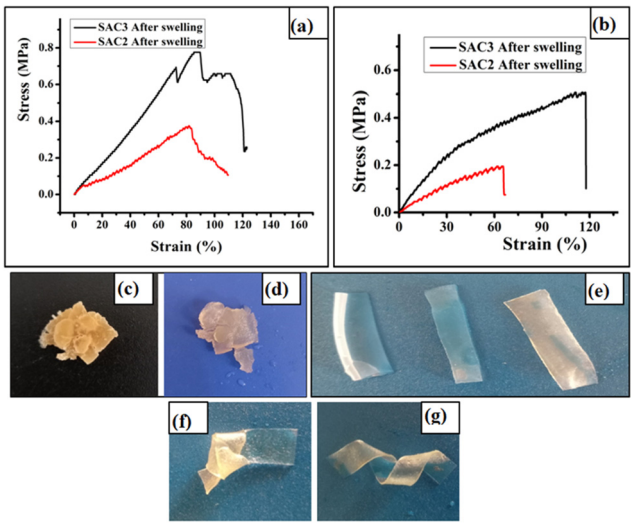

Fig. 4 Mechanical strength of the three compositions of the hydrogel after swelling (a) at 70% water absorption and (b) in the fully swollen state; (c) dried agar gel, (d) swollen agar gel after 7 days swelling in water, (e) digital photographs of the three compositions of the gel after swelling, (f) knot formation of the swollen gel, and (g) bending of the swollen gel.

Drug loading and encapsulation efficiency

In a controlled drug delivery system, drug loading and encapsulation efficiencies are the most important parameters. Fig. 5(a) shows the drug loading and encapsulation efficiencies of the SAC3 hydrogel with different weight percentages of ciprofloxacin. The loading amount of the drug significantly affected the encapsulation efficiency of the hydrogel, with the highest encapsulation efficiency observed in the case of 10% loading. However, the encapsulation efficiency of the hydrogel decreased upon an increase in the amount of the loaded drug.

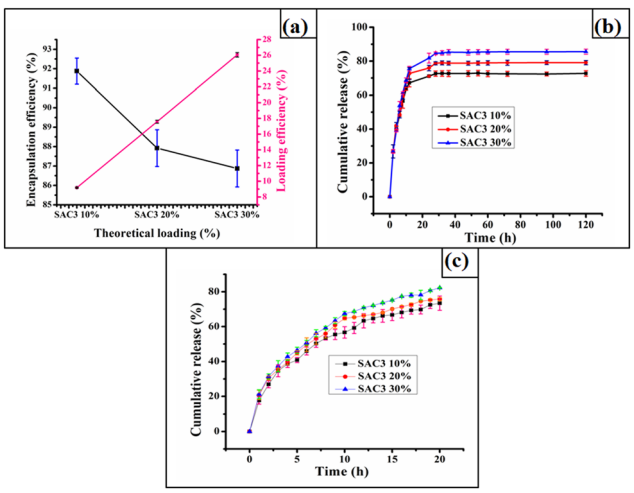

Fig. 5 (a) Drug encapsulation and loading efficiency; cumulative drug release profile over (b) 120 h and (c) 20 h.

This result indicates that, with an increase in the amount of drug loaded in the hydrogel, a greater percentage of the drug was lost during encapsulation.[29]

Drug release

The drug loading efficiency also affected the controlled release ability of the hydrogel, as shown in Fig. 5(b). It was observed that the percentage releasing ability of hydrogel increased with the increase in loading amount and SAC3 with 30% loading showed the highest percentage of release, followed by 20% and 10% loading. This increase in the release amount is mainly due to a diffusion-controlled phenomenon, as the extent of swelling in all the cases was the same. Thus, with the increase in the drug loading, the rate of diffusion increased with the increase in the concentration gradient.[30] In the case of a swellable system, liquid molecules penetrate inside the hydrogel matrix and the drug molecules encapsulated inside the network come out due to Brownian movement. The encapsulated ciprofloxacin exhibited sustained release in all three cases; a property that is one of the most important characteristics for the successful healing of any affected wound. Initially, the drug release rate from the hydrogel was much higher, but the release rate decreased gradually with time, and after 28 h the drug release rate almost reached equilibrium, as shown in Fig. 5(b). Moreover, we also studied the drug release rate over 1 h intervals to investigate the effect of loading amount, as shown in Fig. 5(c).

Moreover, mathematical formulae play an important role in investigating the mechanism of drug release. Suitable mathematical models are important for analyzing quantitative drug release. Usually, the Korsmeyer and Peppas power law expression is used to quantitatively analyze the drug release mechanism of a swellable system. The general empirical equation used to describe the drug release of a swelling system is given by:

$$Q_t/Q_e = Kt^n \quad (8)$$

where Q_t/Q_e is the fractional drug release, Q_e is the equilibrium drug release, and Q_t is the drug release at time t, n is the diffusion exponent, and K is a constant. The value of n is a very important parameter, used to identify the release mechanism.[31–33]

When $n < 0.45$, Fickian diffusion occurs, and the diffusion of the drug plays a predominant role during the release process. If the value of n is equal to 0.85, then swelling plays an important role in drug release. If n is between 0.45 and 0.85, then drug release occurs *via* non-Fickian or an anomalous diffusion mechanism, where both swelling and diffusion processes control the release rate of the drug molecules.

The kinetics data for ciprofloxacin release from the all the variations of the prepared hydrogel were investigated by using this model, as shown in Fig. 6(a). From the metrics, it was observed that the drug release was enhanced with time up to a maximum value and thereafter attained an almost constant value. The data obtained from the slope and intercept of $\ln(Q_t/Q_e)$ *vs.* lnt are given in Table 2. In all cases, values of n

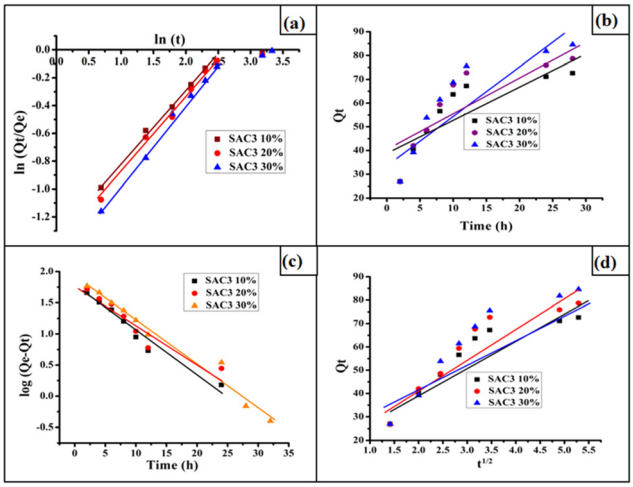

Fig. 6 (a) Korsmeyer and Peppas power law, (b) zero order kinetics, (c) pseudo first order kinetics, and (d) Higuchi square root law at different loadings.

from 0.45 to 0.85 indicate that the drug release occurs *via* non-Fickian diffusion up to almost 70% release, where both diffusion and swelling control the release ability of the drug molecules.

In addition to this, zero order (eqn (9)),[34] Higuchi square root law (eqn (10)),[35] and first order (eqn (11))[36] are empirical relationships for investigating the drug release mechanism, as given below:

$$Q_t = Q_0 + k_0 t \quad (9)$$

$$Q_t = k_2 t^{1/2} \quad (10)$$

$$\log (Q_e - Q_t) = -k_1/2.303t + \log Q_e \quad (11)$$

where Q_t and Q_e are the ciprofloxacin release at certain time (t) and at equilibrium time, respectively, and K_0, K_1, and K_2 are the rate constants.

The plots of data obtained from all the kinetics models are shown in Fig. 6(b) and (d) and the correlation factors are tabulated in Table 2.

Antibacterial activity

After injuries, bacterial infections of the wounded skin are very common and these lead to a delayed healing process and serious tissue damage.[2] Thus, dressing materials should possess a definite amount of antibacterial activity. To investigate

Table 2 Kinetics parameters for drug release systems

Drug release systems	Korsmeyer and Peppas power law		Zero-order R^2 (%)	Pseudo-first order R^2 (%)	Higuchi square root law R^2 (%)
	R^2 (%)	n value			
SAC3 30%	99.40	0.59	70.68	97.20	85.23
SAC3 20%	99.23	0.55	65.94	89.35	81.34
SAC3 10%	99.44	0.51	64.76	95.39	80.66

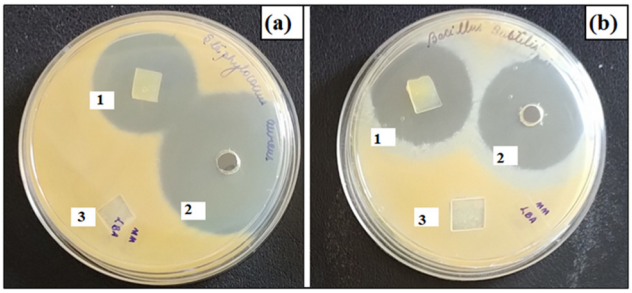

Fig. 7 Antibacterial activity of (1) SAC3 with drug, (2) control, and (3) SAC3 without drug: against (a) SA and (b) BS.

the antibacterial activity of the drug-loaded SAC3, the hydrogel without the drug, ciprofloxacin-loaded hydrogel, and ciprofloxacin solution as a control were placed in separate segments of agar plates. After 24 h, the drug-loaded hydrogel effectively exhibited an inhibition effect against the tested bacterial strains. However, the hydrogel samples without drug encapsulation did not show any antibacterial activity. The zones of inhibition for each bacterial strain are shown in Fig. 7(a) and (b) and the diameters of the inhibition zones are given in Table 3. These results provide supportive information that the drug was successfully loaded with SAC3 and that after encapsulation the hydrogel exhibits antibacterial activity. Thus, the *in vitro* antibacterial studies demonstrated that drug-loaded SAC3 exhibits sustained antibacterial activity against both Gram-positive and Gram-negative bacteria. Hence, the hydrogel can be efficiently used as an antibacterial dressing material for infected wounds.

Biocompatibility testing

Biocompatibility is the most essential property of biomaterials. Favorable cell compatibility is a prerequisite in the design of a biomaterial for wound dressing applications. In this study, to assess biocompatibility, human embryonic kidney cells (HEK 293) were employed against the SAC3 hydrogel without the loading of any drug. Different concentrations of hydrogel samples with this cell type were cultured for 24 h and the results were plotted as shown in Fig. 8(a). The cell viability slightly decreased with the increase in the concentration of the hydrogel, but a minimum 89.46 ± 0.38% cell viability was obtained. Thus, the hydrogel exhibited an acceptable range of cell viability, suggesting that the synthesized hydrogel is non-toxic and can be safely employed as a dressing material for wound healing. Moreover, after treatment with different concentrations of SAC3, the change in cell morphology was also studied with the help of an inverted microscope, as shown in Fig. 8(b) and (d). The cell morphology remained intact after the

Table 3 Inhibition zone diameter of the antibacterial study

Bacterial strain	Inhibition zone diameter for drug loaded hydrogel (mm)	Inhibition zone diameter for control system (mm)
BS	26 ± 4.73	33.67 ± 0.58
SA	32.67 ± 1.15	40 ± 0

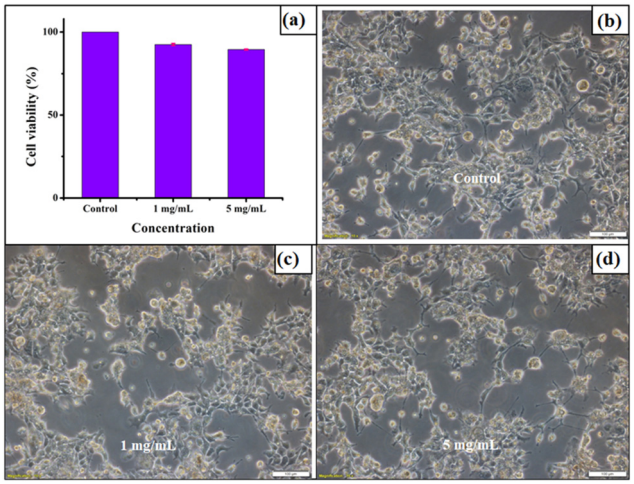

Fig. 8 (a) Cell viability of human embryonic kidney cells (HEK 293) with SAC3 hydrogel; microscopy images of the cells (b) without treatment, and treated with (c) 1 mg mL^{-1} SAC3 and (d) 5 mg mL^{-1} SAC3.

treatment and only a slight difference was observed, indicating the biocompatible nature of the synthesized hydrogel.

Biodegradation

Biodegradation of a polymeric material is an essential property from an environmental point of view. In most cases, dressing materials are removed regularly after certain time intervals and the non-degradability of these can cause serious environmental pollution. Thus, we studied the biodegradation of the synthesized hydrogel. It was seen that the hydrogel was easily degraded by up to 92.33 ± 2.52% within one month when it was buried under the soil (Fig. 9(a)) at our university campus. The micro-organisms present in the soil are responsible for this degradation[37] and the degradation was enhanced due to the absence of synthetic monomers. The SEM images of the oven-dried hydrogel films before and after degradation are shown in Fig. 8(b)–(f). It is seen that the smooth surface of the hydrogel became rough due to the erosion caused by the degradation.

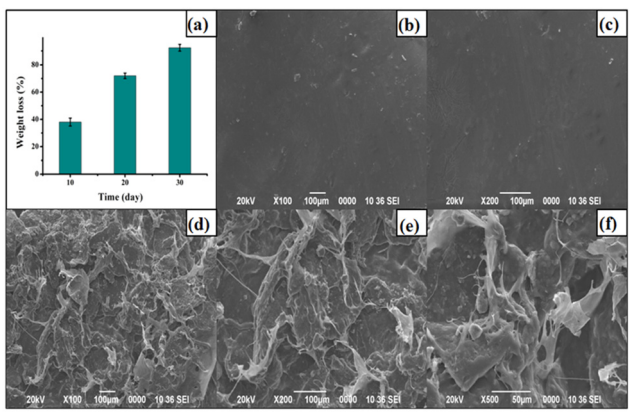

Fig. 9 (a) Weight loss of SAC3 after degradation at various time intervals, (b and c) SEM images of the SAC3 before biodegradation, and (d–f) SEM images of SAC3 after degradation.

Thus, the SEM images provide the supportive information for the biodegradation of the synthesized hydrogels.

Conclusions

In summary, a mechanically tough polysaccharide-based hydrogel was developed without the inclusion of any synthetic monomers. The synthesized hydrogel possesses outstanding mechanical strength (9.49 ± 1.29–6.16 ± 0.37 MPa), making it suitable for wound dressing applications. Moreover, the hydrogel can retain its integrity in the swollen state too, and incredible tensile strength was obtained under such conditions. This property aids the easy removal of the dressing material, meaning that it might be less painful to the host. In addition, the hydrogel exhibits a controlled water transmission rate, which is one of the most important properties of a dressing material. Moreover, the drug-loaded hydrogel exhibited efficient antibacterial activity against the tested bacterial strains. The hydrogels without any drugs also showed good biocompatibility with human embryonic kidney cells (HEK 293) and a minimum 89.46 ± 0.38% cell viability was observed. Above all, the hydrogels exhibit a minimum 86.87 ± 0.95% encapsulation efficiency of the drug with a maximum 85.28 ± 1.58% sustained release ability. Thus, this work details the preparation of a mechanically strong, bio-based, biocompatible hydrogel, which exhibits antibacterial drug release ability upon drug loading and hence can be used as a wound dressing. In conclusion, this work shows promise for the development of polysaccharide-based dressing materials.

Author contributions

Dimpee Sarmah: conceptualization, methodology, writing – original draft preparation, investigation. Munmi Borah: methodology, investigation on bio-related work. Manabendra Mandal: supervision, and validation on bio-related work. Niranjan Karak: supervision, validation, writing – reviewing and editing.

Conflicts of interest

There are no conflicts to declare.

Acknowledgements

The authors want to thank SAIC, Tezpur University, Assam, India for providing analytical facilities.

References

1 R. Xu, H. Xia, W. He, Z. Li, J. Zhao, B. Liu and J. Wu, *Sci. rep.*, 2016, **6**, 1–12.
2 X. Qiu, J. Zhang, L. Cao, Q. Jiao, J. Zhou, L. Yang and Y. Wei, *ACS Appl. Mater. Interfaces*, 2021, **13**, 7060–7069.
3 D. Zhao, J. Huang, Y. Zhong, K. Li, L. Zhang and J. Cai, *Adv. Funct. Mater.*, 2016, **26**, 6279–6287.
4 M. Tavakolian, J. G. Munguia-Lopez, A. Valiei, M. S. Islam, J. M. Kinsella, N. Tufenkji and T. G. van de Ven, *ACS Appl. Mater. Interfaces*, 2020, **12**, 39991–40001.
5 P. Lin, S. Ma, X. Wang and F. Zhou, *Adv. Mater.*, 2015, **27**, 2054–2059.
6 L. Liu, X. Li, M. Nagao, A. L. Elias, R. Narain and H. J. Chung, *Polymers*, 2017, **9**, 558.
7 K. Fang, R. Wang, H. Zhang, L. Zhou, T. Xu, Y. Xiao and J. Fu, *ACS Appl. Mater. Interfaces*, 2020, **12**, 52307–52318.
8 H. Chen, C. Peng, L. Wang, X. Li, M. Yang, H. Liu and W. Chen, *Chem. Eng. J.*, 2021, **403**, 126341.
9 T. Zhu, J. Mao, Y. Cheng, H. Liu, L. Lv, M. Ge and Y. Lai, *Adv. Mater. Interfaces*, 2019, **6**, 1900761.
10 J. G. Lyons, L. M. Geever, M. J. Nugent, J. E. Kennedy and C. L. Higginbotham, *J. Mech. Behav. Biomed. Mater.*, 2009, **2**, 485–493.
11 H. Chen, F. Yang, R. Hu, M. Zhang, B. Ren, X. Gong and J. Zheng, *J. Mater. Chem. B*, 2016, **4**, 5814–5824.
12 H. Itagaki, T. Kurokawa, H. Furukawa, T. Nakajima, Y. Katsumoto and J. P. Gong, *Macromolecules*, 2010, **43**, 9495–9500.
13 T. Wang, D. Liu, C. Lian, S. Zheng, X. Liu and Z. Tong, *Soft Matter*, 2012, **8**, 774–783.
14 D. Sarmah and N. Karak, *J. Cleaner Prod.*, 2022, **344**, 131074.
15 G. Lu, K. Ling, P. Zhao, Z. Xu, C. Deng, H. Zheng and J. Chen, *Wound Repair Regen.*, 2010, **18**, 70–79.
16 P. Wu, A. C. Fisher, P. P. Foo, D. Queen and J. D. S. Gaylor, *Biomaterials*, 1995, **16**, 171–175.
17 A. Saxena, K. Sachin, H. B. Bohidar and A. K. Verma, *Colloids Surf., B*, 2005, **45**, 42–48.
18 A. Heydari, A. Pardakhti and H. Sheibani, *Macromol. Mater. Eng.*, 2017, **302**, 1600501.
19 M. A. Rather, P. J. Deori, K. Gupta, N. Daimary, D. Deka, A. Qureshi and M. Mandal, *Chemosphere*, 2022, **300**, 134497.
20 K. Gupta, S. Barua, S. N. Hazarika, A. K. Manhar, D. Nath, N. Karak and M. Mandal, *RSC Adv.*, 2014, **4**, 52845–52855.
21 H. Mert, B. Özkahraman and H. Damar, *J. Drug Delivery Sci. Technol.*, 2020, **60**, 101962.
22 Y. Song, L. Li and Q. Zheng, *J. Agric. Food Chem.*, 2009, **57**, 2295–2301.
23 D. Sarmah and N. Karak, *Carbohydr. Polym.*, 2020, **242**, 116320.
24 L. Zhang, J. Zhou and L. Zhang, *Carbohydr. Polym.*, 2013, **94**, 386–393.
25 D. Sarmah and N. Karak, *J. Appl. Polym. Sci.*, 2020, **137**, 48495.
26 S. Roy and J. W. Rhim, *Food Hydrocolloids*, 2021, **118**, 106823.
27 J. He, M. Shi, Y. Liang and B. Guo, *Chem. Eng. J.*, 2020, **394**, 124888.
28 R. Wang, N. Li, B. Jiang, J. Li, W. Hong and T. Jiao, *Colloids Surf., A*, 2021, **615**, 126270.
29 S. B. Wang, A. Z. Chen, L. J. Weng, M. Y. Chen and X. L. Xie, *Macromol. Biosci.*, 2004, **4**, 27–30.

30 C. Y. Yu, X. C. Zhang, F. Z. Zhou, X. Z. Zhang, S. X. Cheng and R. X. Zhuo, *Int. J. Pharm.*, 2008, **357**, 15–21.
31 N. Gull, S. M. Khan, O. M. Butt, A. Islam, A. Shah, S. Jabeen and M. T. Z. Butt, *Int. J. Biol. Macromol.*, 2020, **162**, 175–187.
32 D. Pathania, C. Verma, P. Negi, I. Tyagi, M. Asif, N. S. Kumar and V. K. Gupta, *Carbohydr. Polym.*, 2018, **196**, 262–271.
33 T. S. Anirudhan and S. R. Rejeena, *J. Appl. Polym. Sci.*, 2014, 131.
34 S. M. Sreedharan and R. Singh, *Int. J. Nanomed.*, 2019, **14**, 9905–9916.
35 E. Altun, E. Yuca, N. Ekren, D. M. Kalaskar, D. Ficai, G. Dolete and O. Gunduz, *Pharmaceutics*, 2021, **13**, 613.
36 A. Abbas, M. A. Hussain, M. Amin, M. N. Tahir, I. J. antan, A. Hameed and S. N. A. Bukhari, *RSC Adv.*, 2015, **5**, 43440–43448.
37 N. Thombare, S. Mishra, M. Z. Siddiqui, U. Jha, D. Singh and G. R. Mahajan, *Carbohydr. Polym.*, 2018, **185**, 169–178.